Nuclear Interactions of High-Energy μ Mesons in Carbon

I. B. McDiarmid
Division of Pure Physics, National Research Council, Ottawa, Canada
(Received November 15, 1957)

A multiplate cloud chamber containing two large plastic scintillators capable of selecting nuclear interactions is described. Forty-three interactions, attributed to energetic μ mesons, have been observed in the chamber and the following cross sections for interactions in carbon obtained: $(5.6\pm1.1)\times10^{-30}$ cm^2/nucleon for all interactions involving energy transfers >50 Mev and $(1.7\pm0.6)\times10^{-30}$ cm^2/nucleon for shower production. It is shown that several aspects of the interactions can be reasonably accounted for with the aid of the semiclassical Williams-Weizsäcker method and the results are used to infer photon interaction cross sections in carbon for photon energies up to about 10 Bev. The μ-meson cross sections reported here are in agreement with those found by George and Evans using emulsion techniques, but some of the details of the interactions differ and it is suggested that an appreciable fraction of the stars observed in an emulsion exposed underground may be due to π mesons or protons.

INTRODUCTION

NUCLEAR interactions produced in photographic emulsions exposed underground were first reported by George and Evans.[1] Since the μ meson is the only known particle capable of penetrating to appreciable depths underground, George and Evans attributed all $1p$ stars and showers to these particles and found that the measured cross sections could be understood with the aid of the Williams-Weizsäcker virtual photon method and the experimentally known (at low energies) photon cross section. Other than the work of these authors only a small number of observations have been reported on the nuclear interactions of fast μ mesons. A few underground multiplate cloud chamber experiments[2–4] have detected showers presumably produced by μ mesons and have given cross sections falling in the range $(0.5$ to $3.2)\times10^{-30}$ cm^2/nucleon. On the other hand, the lower energy interactions not involving π-meson production have been observed only in photographic emulsions. Furthermore, it has not been shown directly, in either the emulsion or the cloud chamber work, that the particles responsible for the interactions were in fact μ mesons.

The purpose of the experiment reported here was to examine in some detail and by a different method interactions produced by fast particles most of which could be shown to be μ mesons. Since the interactions were studied in a cloud chamber and since the μ-meson cross section is rather small (10^3–10^4 times smaller than for π mesons) it was necessary to employ an efficient selection system biased strongly against unwanted events; for this purpose a Geiger telescope in coincidence with a combination of two scintillators was used. This arrangement with slight modifications could be used to select other "rare" events.

EXPERIMENTAL METHOD

The experiment was performed under a 90-cm thick lead absorber at sea level. The cloud chamber, of inside dimensions $70\times50\times30$ cm, contained nine 1.27-cm lead plates and two 3.18-cm thick plastic scintillators; the arrangement is shown schematically in Fig. 1. The chamber itself was of relatively simple construction consisting of a central box-like casting open on four sides. Two sides were closed with plate glass through which the chamber was illuminated and photographs taken. The piston formed the third side and the fourth was a metal plate through which passed two light pipes from the scintillators and on which photomultipliers were mounted. The chamber was illuminated by two flash tubes mounted behind cylindrical lenses on one side of the chamber. A mirror on the opposite side

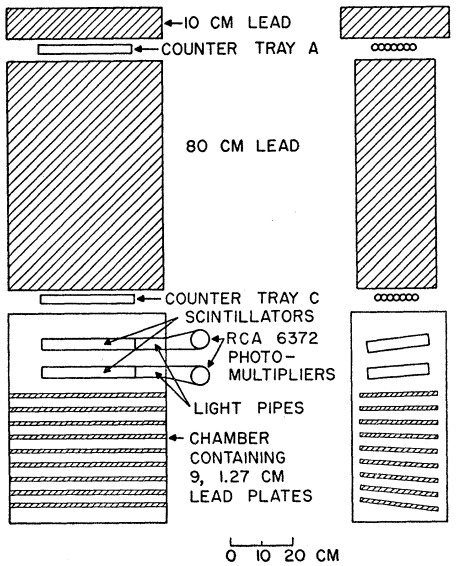

FIG. 1. Experimental arrangement.

[1] E. P. George and J. Evans, Proc. Phys. Soc. (London) **A63**, 1248 (1950); **A68**, 829 (1955); E. P. George, in *Progress in Cosmic Ray Physics*, edited by J. G. Wilson (North Holland Publishing Company, Amsterdam, 1952), Vol 1, Chap. VII.
[2] Lovati, Mura, Succi, and Tagliaferri, Nuovo cimento **10**, 1201 (1953).
[3] H. J. J. Braddick and B. Leontic, Phil. Mag. **45**, 1287 (1954).
[4] Higashi, Oshio, Shibata, Watanabe, and Watase, Nuovo cimento **5**, 592 (1957).

reflected the light back on itself and thin aluminum sheets fixed to the surface of the plates improved the uniformity of illumination.

Photographs were taken with two cameras, one mounted centrally on the axis of the chamber and one 15° off the axis. The camera assembly was mounted rigidly on a steel plate which could be positioned accurately and moved easily. Photographs were reprojected with the original cameras through a glass plate identical to the front glass of the chamber. The film was repositioned in the cameras by means of fiduciary marks imaged on the film at the time of exposure. The reprojection procedure was similar to the method described by Hodson *et al.*[5] in which two orthogonal projections of each event are drawn. Spatial reconstruction of average tracks in this way was accurate to about ± 1 mm for the depth coordinate and slightly better than this for the other two coordinates. Projected angles of scattering in the lead plates were used for momentum estimates and these were measured using the photograph taken with the centrally mounted camera by projecting the track on a rotatable screen as described previously.[6] The measured "noise level" scattering[6] was 0.35 degree corresponding to a maximum detectable momentum, as defined by Annis *et al.*[7] of 3.5 Bev.

The plastic (polyvinyltoluene) scintillators, of dimensions $30.5\times19\times3.18$ cm, served three purposes. They were used as carbon targets, as part of the selection system, and to estimate energies of low-energy protons. The scintillator thickness was chosen so that a 20-Mev proton stopping in the scintillator gave a pulse approximately twice that of a relativistic particle passing vertically through. The scintillators were mounted in the chamber in a gas tight aluminum case of thickness $\frac{3}{32}$ in. and light pipes (also polyvinyltoluene) of constant cross-sectional area attached to one end carried the light to RCA 6372 photomultipliers mounted outside the chamber (Fig. 1). The 6372 has a side photo cathode with area approximately equal to the cross-sectional area of a scintillator. This condition, as well as others discussed in detail by Brini *et al.*[8] must be satisfied if a reasonable light yield and a maximum uniformity of response with position are to be obtained with a large scintillator. The response of the scintillators as a function of position was determined by scanning the surface with a pencil beam of γ rays and measuring the photomultiplier current with a galvanometer. Lines of equal response were drawn for each scintillator and these were used to correct pulses due to particles whose position could be determined from the cloud chamber photographs. The maximum variation with position was approximately $\pm 13\%$ and this considerably

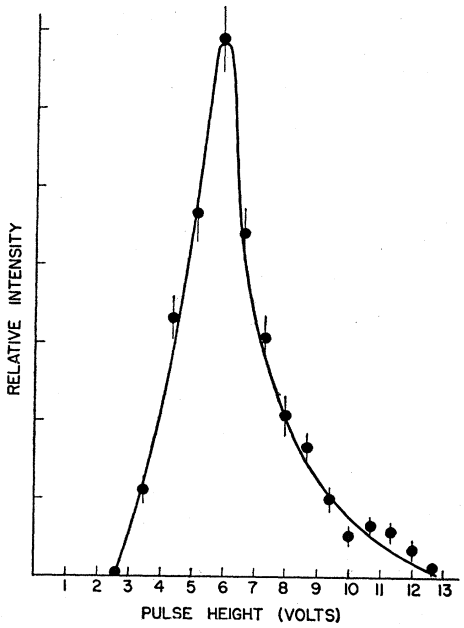

FIG. 2. Pulse-height distribution for near-vertical μ mesons.

broadened the pulse-height distribution for relativistic particles. The pulse-height distribution is given in Fig. 2 for near-vertical μ mesons incident uniformly over the surface of the scintillator and the width of the distribution is about twice that expected from Symon's theory[9] owing to ionization fluctuations. Most of the additional spread can be attributed to the variation of response with position, but an appreciable contribution to the number of large pulses also comes from knock-on electrons from the lead absorber accompanying the μ mesons.

Since the response of plastic scintillators to nonrelativistic particles is nonlinear it was necessary to carry out a calibration before proton energies could be estimated from the pulse heights. Birks' theory[10] for organic scintillators relates dV/dr, the light output/(g/cm^2) to dE/dr, the specific ionization of the particle by means of the expression

$$\frac{dV}{dr}=\frac{C(dE/dr)}{1+KB(dE/dr)}, \tag{1}$$

where C is a constant and KB a parameter depending on the scintillator. In the limit of low ionization (electrons) Eq. (1) predicts a light output proportional to the energy of the particle (or to the energy loss if the particle passes through) while for high specific ionization the light output is proportional to the range of the particle in the scintillator. These relations have been checked for the scintillators used here and the

[5] Hodson, Ballam, Arnold, Harris, Rau, Reynolds, and Treiman, Phys. Rev. **96**, 1089 (1954).
[6] I. B. McDiarmid, Phil. Mag. **45**, 933 (1954).
[7] Annis, Bridge, and Olbert, Phys. Rev. **89**, 1216 (1953).
[8] Brini, Peli, Rimondi, and Veronesi, Nuovo cimento **2**, 10 (1955).
[9] K. R. Symon, quoted in B. Rossi, *High-Energy Particles* (Prentice-Hall, Inc., Englewood Cliffs, New Jersey, 1952), p. 32.
[10] J. B. Birks, *Scintillation Counters* (Pergamon Press Ltd., London, 1953), p. 93.

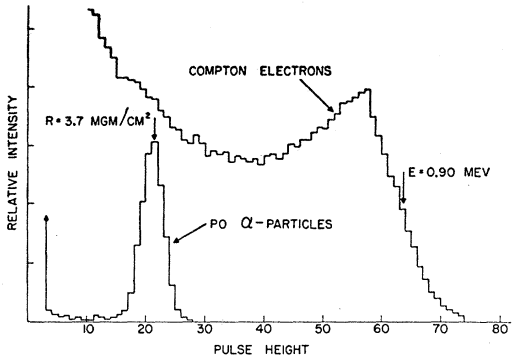

FIG. 3. Pulse-height distribution for Po α particles (residual range in scintillator = 3.7 mg/cm²) and Compton Electrons produced by a Zn^{65} γ-ray source (maximum Compton energy = 0.90 Mev).

value of KB determined. An identical plastic scintillator, in the form of a cylinder of diameter 2 in. and height $1\frac{1}{4}$ in., was mounted on the end of an RCA 5819 phototube and a 20-channel pulse-height analyser was used to determine pulse-height distributions for the Compton electrons produced by several γ-ray sources. Distributions were also obtained for Po α particles corresponding to different residual ranges in the scintillator. Two typical distributions are given in Fig. 3 where the numbers affixed to the arrows give the maximum Compton energy of the electrons and the residual range of the α particles, the positions of the arrows indicate the pulse-height associated with the corresponding energy or range. In Fig. 4 pulse heights are plotted against maximum Compton energy for the electrons and against range in the scintillator for the α particles, quite a good linear relationship being obtained in each case. The parameter KB, characteristic of the scintillators used here, is equal to the ratio of the slopes of the electron and α-particle lines drawn in Fig. 4 and was found to be 12.6 ± 1.6 (mg/cm²)/Mev. This value of KB was used in Eq. (1), along with calculated values of dE/dr,[11] to estimate proton energies.

The schematic diagram in Fig. 5 shows the components of the selection system and the method of recording the scintillator pulse heights. During the operating time the scaler continuously recorded the number of acceptable μ mesons which passed through the apparatus. The bias settings on discriminators 1, 2, 3, and 4 were 28, 9, 9, and 38 volts, respectively (most probable pulse of a vertical μ meson was 6 volts, Fig. 2). The cloud chamber was expanded and the pulses recorded when either of two selection criteria was satisfied; the first of these was

$$A+C+[(T+B>28\text{ v})+(T \text{ or } B<9\text{ v})],$$

where T and B refer to pulse size from top and bottom scintillator. This selected, among other things, events in which a μ meson passed through both scintillators and produced a nuclear interaction in one giving a pulse $\gtrsim 16$ volts, provided none of the secondaries entered the other scintillator. Hence, events in which energetic π mesons were produced were efficiently selected only if they occurred in the bottom scintillator while lower energy events occurring in both scintillators were detected. The selection efficiency for different events is discussed more fully below.

Other events selected included μ mesons stopping, particularly in the top scintillator, and electronic events most of which consisted of two or three electrons which accompanied the μ meson and stopped in the top scintillator. These latter events made up approximately 60% of all those selected with this system. With the arrangement shown in Fig. 1 the rate of acceptable μ mesons through the apparatus was 495/hr while the rate at which pictures were taken was 0.5/hr. The fraction of useful pictures obtained was therefore increased by approximately a factor 1000 compared to a selection system consisting of a simple Geiger telescope.

The second selection criterion was

$$A+C+(B>38\text{ v}).$$

Events selected by this system and not by the first included large interactions in the top scintillator, large interactions from the lead above the chamber, and μ mesons accompanied by at least 5 or 6 electrons which penetrated both scintillators. Again, these latter events made up about 90% of the total. The photography rate for this system was also 0.5/hr giving an over-all rate of $\sim$1/hr.

If the bias is set at 22 volts instead of 38 volts, the second selection system accepts the same interactions occurring in the bottom scintillator as does the first system. However, the rate corresponding to such a selection is about six times that of the first system, the additional events being mostly μ mesons accompanied by 2 or 3 electrons which penetrate both scintillators. Therefore, the fraction of useful pictures obtained with

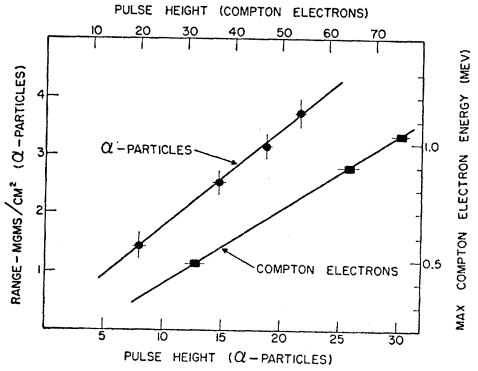

FIG. 4. Pulse heights plotted against range for α particles and against maximum energy for Compton electrons produced by C^{137}, Zn^{65}, and Co^{60} γ-ray sources.

[11] H. A. Bethe, in *Experimental Nuclear Physics*, edited by E. Segrè (John Wiley and Sons, Inc., New York, 1953), Vol. I, Part II.

the first selection system was approximately six times that obtained with a system consisting of a Geiger telescope and one scintillator biased to select the same events.

RESULTS

a. Classification of Events

5178 photographs have been taken corresponding to 1.9×10^6 traversals, by charged particles, of the Geiger telescope and both scintillators. Those photographs were selected in which a single unaccompanied particle at minimum ionization entered the chamber and produced a pulse in one scintillator $\gtrsim 20$ volts (approximately the minimum requirements of the first selection system). In all cases, what appeared to be the original particle was present after the interaction and penetrated several lead plates. Most of the events were cases in which the incident particle produced electrons in one of the scintillators; the remainder of those selected could be classified as follows:

(1) Fifteen events in which at least one penetrating secondary (penetrated more than two plates without multiplying) was produced by the incident particle in one of the scintillators [Fig. 6(a), 6(b)] or the top lead plate [Fig. 6(c)]. These were obvious cases of nuclear interactions.

(2) Fifteen events in which at least one heavily ionizing particle and no secondary penetrating particles emerged from the scintillator [Fig. 6(d)]. These were either nuclear interactions or elastic Coulomb collisions between the incident particle and a hydrogen nucleus in the scintillator.

(3) Eighty-two events in which no visible secondaries emerged from the scintillators. These were either nuclear interactions, elastic collisions with hydrogen, or electronic events in which the electrons did not emerge from the scintillator.

All the above events were reprojected to determine the spatial angles of the particles after the interaction with respect to the primary direction and the distances

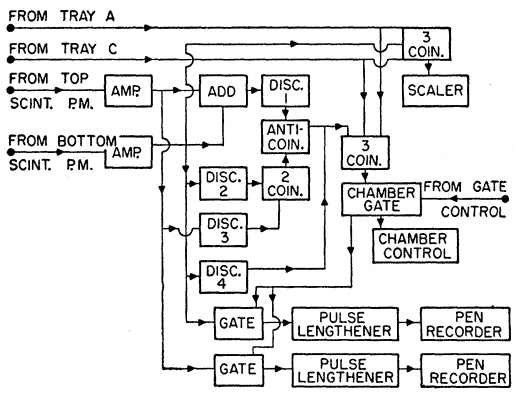

FIG. 5. Schematic diagram of the circuits.

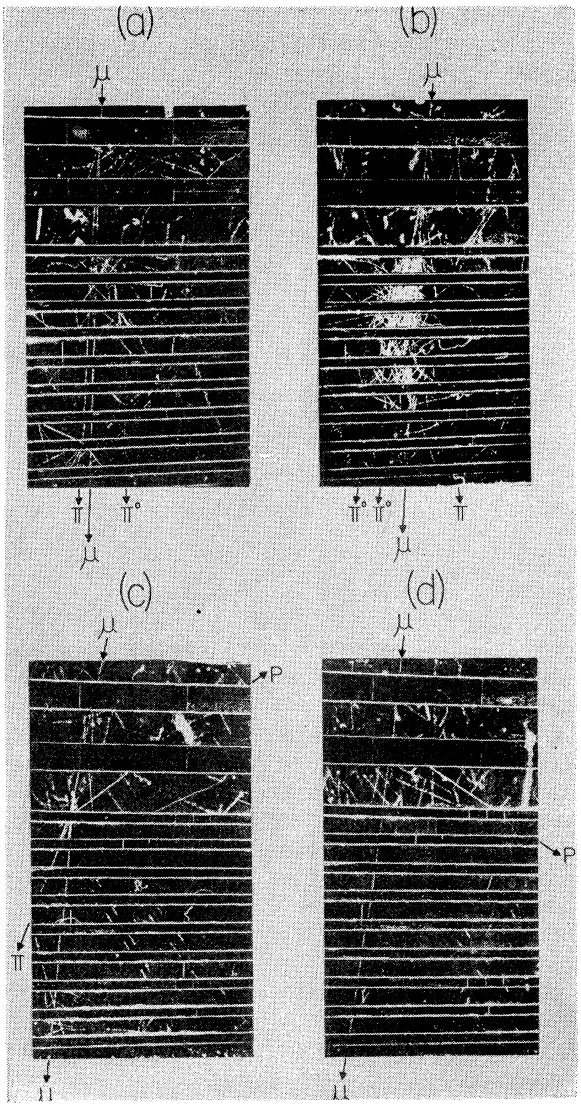

FIG. 6. Examples of nuclear interactions produced by μ mesons. (a) Interaction in the top scintillator in which one charged and one neutral π meson are produced. The charged meson interacts in the eighth plate. The third charged particle coming from the top scintillator is an electron, presumably a knock-on. (b) Interaction in the bottom scintillator in which at least one charged and two neutral mesons are produced. The energy in the electron showers ≈ 9 Bev. (c) Interaction in the top plate in which one π meson and several protons are emitted, one proton enters the bottom scintillator. (d) Interaction in the bottom scintillator in which a single proton emerges.

travelled in the scintillators by the emerging particles. The position at which events occurred in the scintillator was noted and the pulse height corrected using the response *vs* position measurements referred to above. Momentum estimates were made either from the range of particles stopping in the plates or from the rms scattering angle when this could be measured.

Upper and lower limits to the energy of the heavily ionizing particles in group (2), assumed to be protons,

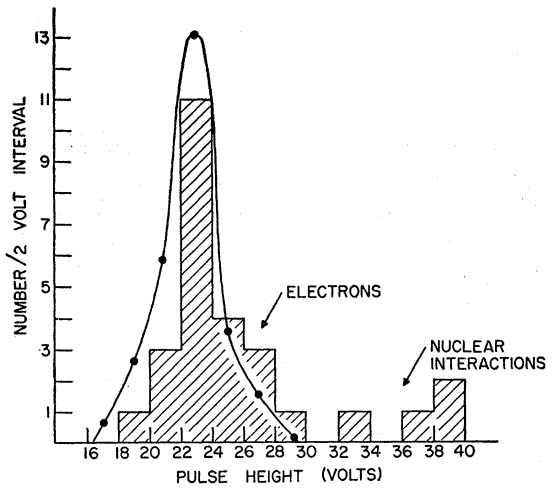

FIG. 7. Pulse-height distribution in the bottom scintillator for events in which the primary particle was not scattered and no secondary particles emerged from the scintillator. The smooth curve is the measured distribution for events which could be identified as electronic.

could usually be determined from the distance travelled in the target scintillator and the fact that generally they stopped either in the other scintillator or the first plate. The energy of the secondary could also be estimated from the pulse height; if the two estimates were inconsistent it was assumed that other secondary ionizing particles stopped in the scintillator. In all but five cases the range and pulse-height measurements were inconsistent with the production of a single secondary particle, hence these could not be elastic collisions with hydrogen. The five remaining cases were shown to be inconsistent with the dynamics of a $\mu-p$ collision and therefore all events in group (2) were assumed to be nuclear interactions.

Events in group (3) were used in the analysis only if the large pulse occurred in the bottom scintillator, this was because small distortions sometimes occurred in the chamber above the top scintillator making angle measurements rather uncertain. These events were further divided into two groups; 27 in which there was no measurable scattering of the incident particle in the bottom scintillator and 14 in which a deflection $\gtrsim 1.5°$ occurred. If the events in which the incident particle was not scattered were electronic (the others obviously were not) it is likely that they were cases in which one or more electrons (knock-on's or electron pairs) were produced in the upper case of the bottom scintillator. Therefore, the pulse height distribution for these, given by the histogram in Fig. 7, should be the same as that for electrons entering the bottom scintillator from the lower case of the top. Also, the number of events should be approximately equal to the number of cases in which electrons from the case of the top scintillator enter the bottom but do not emerge from it. The smooth curve in Fig. 7 is the pulse-height distribution, in the bottom scintillator, for 70 cases in which electrons were produced in the lower case of the top scintillator, normalized to represent the same number of events as the histogram. Out of the 70 events there was none with a pulse height >29 volts and it is evident from Fig. 7 that the agreement between the two distributions is reasonable up to 29 volts. Hence it was assumed that the 23 events in this group with pulse height <30 volts were electronic and that the remaining 4 were nonelectronic. In 18 of the 70 cases in which electrons were produced in the case of the top scintillator, no electrons emerged from the bottom scintillator; this number agrees well with the above estimated number of electronic events in group (3).

In 13 of the 18 nonelectronic events in group (3) the measurements of pulse height, angle of deflection and momentum of the incident particle were inconsistent with the dynamics of an elastic $\mu-p$ collision and in 3 cases they were inconclusive. In 2 cases the measurements were consistent with an elastic collision and since this is approximately the number expected from the Rutherford formula (in which the proton receives an energy >20 Mev) it was assumed that the remaining 16 events were nuclear interactions.

From the foregoing the total number of nuclear interactions recorded, not counting those in group (3) occurring in the top scintillator, was 46, of which 9 occurred in the top scintillator, 32 in the bottom and 5 in the first lead plate [these were selected if a proton was emitted backwards from the plate to the scintillator, Fig. 6(c)]. The requirements of the first selection system set a lower limit of approximately 20 Mev for single protons emitted in an interaction and a slightly higher limit if more than one proton or one or more α particles were emitted. Assuming that neutrons carry away an equal amount of energy it was estimated that only interactions in which the energy transfer to the nucleus was $\gtrsim 50$ Mev were detected.

For cross-section determinations only interactions occurring in the bottom scintillator were used and generally it was possible to use the pulse in the top scintillator as an additional check that only a single relativistic particle entered the chamber. The requirements of the first selection system meant that interactions were missed if the primary was accompanied by a knock-on electron or if a proton from an interaction in the bottom scintillator entered the top. An upper limit of 14% for the inefficiency caused by these effects was obtained from the area above 9 volts in the pulse-height distribution in Fig. 2 and from the number of interactions detected in the top plate in which a proton was emitted back to the bottom scintillator. Hence it was assumed that interactions in the bottom scintillator corresponding to energy transfers $\gtrsim 50$ Mev were detected with an efficiency of approximately 90%. Events involving the emission of a single π meson not accompanied by a break-up of the carbon nucleus would also be missed, this being particularly true of π^0 emis-

sion. If an inefficiency arises due to this it likely applies only to a fairly small range of energy transfers; i.e., 150 to perhaps 300 Mev.

b. μ-Meson Cross Sections

It was assumed that the interactions were produced by a mixture of μ mesons and π mesons and the number of π mesons determined from the number of interactions produced by the primary on traversing the lead plates. For interactions in groups (2) and (3) there was only one penetrating particle and this was assumed to be the primary. For interactions in group (1) there were at least two penetrating particles; the primary after the interaction was taken to be the one making the smallest angle with the incident direction, this being a reasonable assumption for the case of μ-meson induced interactions. If the identification of the primary after the interaction is incorrect then the number of incident π mesons will be over estimated and the μ-meson cross section under estimated. In the 46 nuclear interactions observed in the scintillators or the first plate a total of 4850 (g/cm^2) of lead was traversed by the primary after the interaction; in three cases in group (3) the particle produced a second interaction in one of the plates and in no case was a large-angle scattering event observed. If one assumes that the three interactions were due to π mesons, the ratio of π-induced to μ-induced interactions in the scintillators was $N_i\lambda_{\pi p}/t$, where $N_i=3$, $t=4850$ g/cm^2, and $\lambda_{\pi p}$ is the interaction length (interactions and large angle scatter) for π mesons in lead, taken to be 174 g/cm^2.[12] This gave a ratio of $10\pm6\%$; hence it was concluded that if the 3 cases in which the primary produced a second interaction in the plates were omitted, more than 95% of the remaining nuclear interactions were produced by μ mesons.

An alternative way to see the effect of π mesons and also determine the μ-meson cross section is given by the following relations:

$$N_1=\epsilon\left(\frac{N_\pi t_s}{\lambda_{\pi s}}+\frac{N_\mu t_s}{\lambda_\mu}\right), \tag{2}$$

$$N_2=\epsilon F\left(\frac{N_\pi t_p}{\lambda_{\pi p}}+\frac{N_\mu t_p}{\lambda_\mu}\right), \tag{3}$$

$$N_3=\epsilon\left[\left(\frac{t_s}{\lambda_{\pi s}}+\frac{0.6t_s}{\lambda_{\pi s}}+\frac{Ft_p}{\lambda_{\pi p}}\right)\frac{N_\pi \bar{t}_p}{\lambda_{\pi p}}+\text{term}\propto 1/\lambda_\mu{}^2\right], \tag{4}$$

where N_1, N_2, N_3 are the numbers of interactions produced by primaries in the bottom scintillator (32), in the first plate (5) and in the remaining plates (3), respectively. N_μ and N_π are the numbers of incident μ mesons and π mesons, respectively. $(N_\mu+N_\pi)=1.9\times10^6$. $\lambda_{\pi s}$ and $\lambda_{\pi p}$ are the interaction lengths for π mesons in the scintillator (81 g/cm^2) and in the lead (174 g/cm^2).[12] λ_μ is the interaction length for μ mesons. t_s and t_p are the thicknesses of the scintillator and case (5.05 g/cm^2) and one lead plate (14.4 g/cm^2). $\bar{t}_p$ is the average thickness of lead traversed by a primary after an interaction (107 g/cm^2). ϵ is the detection efficiency in the bottom scintillator (0.9). F is the fraction of all the interactions in the first plate in which a proton is emitted back into the bottom scintillator. The factor 0.6 in Eq. (4) is the efficiency of the top scintillator relative to the bottom for detecting nuclear interactions, determined from the ratio of the numbers observed in each.

An upper limit for N_π of 570 is obtained if it is assumed that all the interactions in the bottom scintillator were produced by π mesons while a lower limit for λ_μ of 2.7×10^5 g/cm^2 is given by assuming all interactions were produced by μ mesons. Therefore, N_μ can be set equal to 1.9×10^6 and the term proportional to $1/\lambda_\mu{}^2$ in Eq. (4) can be neglected. Solving for N_π, λ_μ, and F gives $N_\pi=53\pm30$, $\sigma_\mu=1/(N\lambda_\mu)=(5.6\pm1.1)\times10^{-30}$ cm^2/nucleon, (N=Avogadro's number) $F\approx0.06$. From the fraction of cases in which π mesons were produced a cross section of $(1.7\pm0.6)\times10^{-30}$ cm^2/nucleon is obtained for this process, this value being in good agreement with that found by George and Evans.[1] As discussed above, the value of F was taken as an upper limit for the fraction of interactions missed in the bottom scintillator because a proton was emitted back into the top scintillator.

From the preceding it is concluded that the single unaccompanied particles emerging from a 90-cm lead absorber at sea level include a small fraction of π mesons, the ratio of π mesons to μ mesons being $(2.8\pm1.6)\times10^{-5}$. However, this small fraction of π mesons still accounts for approximately 10% of all the nuclear interactions produced by these particles.

It is also of interest to determine the fraction of all particles (not just unaccompanied particles) emerging from the absorber that are π mesons or protons. A lower limit can be obtained from the number of such shower particles observed to come from the absorber; these events were detected by the second selection system with an efficiency considerably less than 100%. The lower limit found was $N_\pi/N_\mu>19\times10^{-5}$. If the observed showers were initiated by μ mesons, this limit would also apply to the particles detected in a nuclear emulsion exposed underground. However, the sea level flux contains a small fraction of protons[13] and it is estimated that approximately $\frac{1}{3}$ of the showers were due to these particles. Another estimate of N_π/N_μ, applicable to the underground flux, as well as the ratio of π-induced to μ-induced interactions expected in an emulsion exposed underground can be obtained as follows: the number P of charged π mesons produced per g/cm^2 by a μ meson $\approx2\times10^{-6}$, determined from the 17 charged shower particles (not counting μ mesons)

[12] M. S. Sinha and N. C. Das, Phys. Rev. **105**, 1587 (1957).

[13] M. G. Mylroi and J. G. Wilson, Proc. Phys. Soc. (London) **A64**, 404 (1951).

in the interactions in the bottom scintillator. Neglecting decay and ionization loss $N_\pi/N_\mu = P\lambda_{\pi\ \mathrm{ab}}$, where $\lambda_{\pi\ \mathrm{ab}}$ is the π-meson absorption length in the ground, and the ratio of π-induced to μ-induced interactions expected in an emulsion $= P\lambda_{\pi\ \mathrm{ab}}\lambda_\mu/\lambda_{\pi e}$ where $\lambda_{\pi e}$ is the π-meson interaction length in an emulsion. Setting $\lambda_{\pi\ \mathrm{ab}} = \lambda_{\pi e}$ and using the previously determined value of λ_μ gives a ratio ≈ 0.6. This value applies to a depth of a few π-meson absorption lengths underground, if the μ-meson cross section increases slowly with energy, as it probably does, then the above ratio will increase with depth. Hence, it is concluded that an appreciable fraction of the interactions observed underground by George and Evans[1] and attributed to μ mesons were probably due to π mesons, this conclusion being in agreement with recent calculations of Kitamura and Oda.[14]

c. Nature of the Interactions

The nuclear interactions observed in the present experiment and attributed to μ mesons can now be examined in more detail. The charged shower particles in the interactions in group (1) (omitting the least scattered particle) traversed a total of 1610 g/cm^2 of lead and produced 5 nuclear interactions and 3 large angle scatters. This gives an interaction length 200 ± 70 g/cm^2 which is consistent with these being π mesons. The least scattered particles traversed a thickness of 1590 g/cm^2 of lead and no interactions or large angle scatters were observed this being consistent with the assumption that these were the original μ mesons. The ratio of neutral to charged mesons in the shower particles was 0.22 which is expected to be a lower limit since the probability of missing a π^0 meson of energy <300 Mev is rather large. It was possible to estimate the energy of 25 out of the 38 charged and neutral shower particles observed and a mean value of about 1 Bev was found.

Since μ mesons are not strongly coupled to nucleons, it was suggested by George and Evans[1] that nuclear interactions produced by energetic μ mesons could be accounted for with the aid of the well-known Williams-Weizsäcker[15] (W-W) method. This procedure associates the following virtual photon spectrum with the field of a charged particle of energy E and mass m

$$N(E,K)dK = \frac{2\alpha}{\pi}\frac{dK}{K}\left[\ln\frac{E\hbar c}{Kmc^2 b_m} - 0.39\right], \qquad (5)$$

where K is the virtual photon energy, α is the fine structure constant, and b_m is the minimum distance for which the field of the particle is effective in a given process, taken equal to the proton "radius",[16] 0.77 $\times 10^{-13}$ cm in this work. Equation (5) was averaged over the seal level μ-meson spectrum[17] under 90 cm of lead to give the average virtual photon spectrum $\bar{N}(K)$ per μ meson. The μ-meson cross section for this spectrum and for an energy transfer K is then given by

$$\sigma_\mu(K)dK = \sigma_{\mathrm{ph}}(K)\bar{N}(K)dK, \qquad (6)$$

where $\sigma_{\mathrm{ph}}(K)$ is the photon cross section at energy K for the process in question. If $\sigma_{\mathrm{ph}}(K)$ is known, Eq. (6) can be integrated over K to give the total μ-meson cross section. Recently Kessler and Kessler[18] have discussed the validity of the W-W method and have confirmed the applicability of the method to the problem of the nuclear interactions of μ mesons. These authors also discuss the expected angular deviation of the μ meson in a nuclear interaction and show that a μ meson of energy E transferring an energy K in an interaction has a rather broad scattering angle distribution with mean angle $\bar{\theta} = (K/E)\ \ln^{-1}(E/m)$. For large μ-meson energies this expression predicts rather small angular deviations; however, this is in accord with the W-W method which shows that the virtual photons travel mainly in the direction of the μ meson and hence interactions involving large traverse energy transfers are unlikely. An approximate theoretical angular distribution, applicable to the present results, has been obtained by combining the expression for $\bar{\theta}$ with an energy transfer distribution obtained from Eq. (5) (assuming σ_{ph} constant) and then averaging this distribution over the μ-meson spectrum. In Fig. 8 the angular distribution obtained in this way is compared with the measured distribution. The histogram in Fig. 8(a) refers to all the nuclear interactions

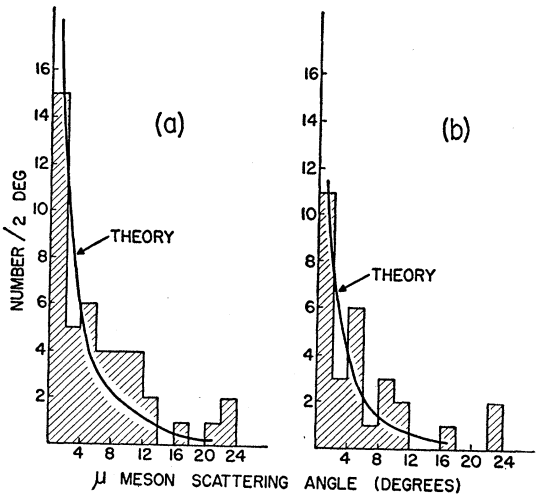

FIG. 8. Distribution of the angular deflections of μ mesons producing nuclear interactions. (a) All interactions. (b) Interactions not involving π-meson production.

[14] T. Kitamura and M. Oda, Progr. Theoret. Phys. Japan **16**, 250 (1956).
[15] E. J. Williams, Kgl. Danske Videnskab. Selskab, Mat.-fys. Medd. **13**, 4 (1935); K. F. Weizsäcker, Z. Physik **88**, 612 (1934).
[16] E. E. Chambers and R. Hofstadter, Phys. Rev. **103**, 1454 (1956).
[17] B. G. Owen and J. G. Wilson, Proc. Phys. Soc. (London) **A68**, 409 (1955).
[18] D. Kessler and P. Kessler, Nuovo cimento **4**, 601 (1956).

attributed to μ mesons while Fig. 8(b) refers to those not involving π-meson production; in both cases the curves have been normalized to represent the number of events in the histograms. Evidently the agreement between the theoretical and measured distributions is reasonable and this is taken as a further indication that the interactions can be accounted for in terms of the W-W theory.

Another quantity which can be measured and whose distribution can be compared with that expected from the W-W theory is the energy transfer in an interaction. Again, for this purpose only interactions occurring in the bottom scintillator could be used. The energy transfer for interactions not involving π-meson production was estimated from the pulse height and the range of the secondary particles (if they emerged from the scintillator). Twice the energy thus obtained was taken as the energy transfer since it was assumed that half the energy was given to neutrons. For interactions involving π-meson production the energy transfer was taken as the sum of the energies of the charged and neutral π mesons. In some cases the charged π mesons left the chamber before traversing enough plates to allow a measurement of the mean scattering angle and for these the mean energy of 1 Bev mentioned above was assumed. The estimated energy transfers are very approximate, the best cases involving uncertainties of $\pm 30\%$; however, it is unlikely that they have been appreciably overestimated since errors due to secondary particles escaping detection in the high-energy events or to α particles contributing to the pulses in the low-energy events will tend to underestimate the energy.

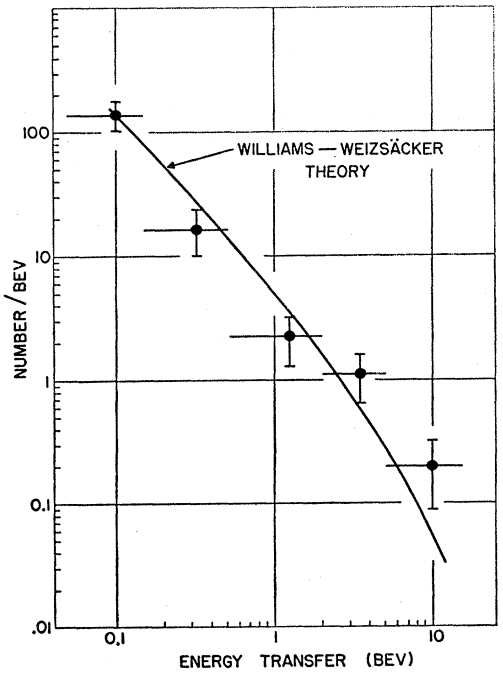

FIG. 9. Energy transfer distribution.

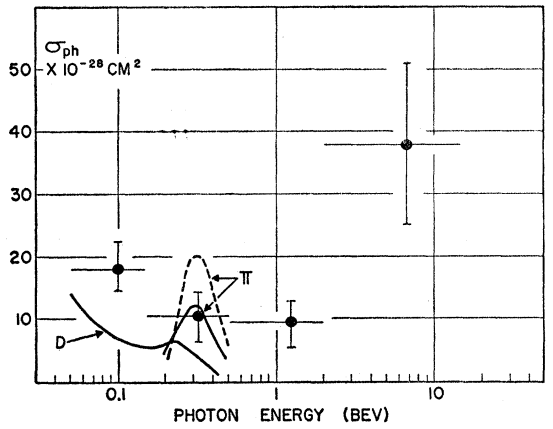

FIG. 10. Total photon interaction cross section as a function of energy in carbon.

The energy transfers were grouped into five energy intervals and the number occurring in each was divided by the width of the interval in Bev; the results are shown in Fig. 9 where the points represent the average number/Bev in the energy intervals indicated by the horizontal lines. The curve in Fig. 9 is $\bar{N}(K)$ normalized to the point at 0.1 Bev this being the energy transfer distribution expected from the W-W method assuming σ_{ph} is independent of energy. Again it is evident that the measurements are consistent with the predictions of the W-W theory if it is assumed that σ_{ph} is nearly constant.

George[1] used the energy release as measured in an emulsion along with the scattering angle of the primary to estimate the energy of the primary in type $1p$ stars. It was assumed that the incident particle suffered an elastic collision with a proton which on recoiling caused the parent nucleus to evaporate. From this and the conservation of energy and momentum a spectrum of the primaries was obtained which agreed with the known spectrum of μ mesons underground. The assumption of an elastic collision with a single proton and the application of the conservation laws is inconsistent with an explanation of the interactions in terms of the W-W method. The fact that agreement was found with the μ-meson spectrum means that scattering angles larger than expected from the W-W method were present and, as pointed out by Kessler and Kessler,[18] this suggests the presence of π mesons or protons among the star primaries. The same analysis as used by George was applied to the interactions (not involving π-meson production) observed in the cloud chamber; the results are shown in Table I in which the number of primary particles found at different energies is compared with the results of George. It can be seen that the two distributions disagree, and in fact the μ-meson spectrum thus obtained for the present experiment differs greatly from the known sea-level spectrum. These results indicate first, that the lower energy interactions do not involve an elastic process and secondly that an appre-

TABLE I. μ-meson energy spectra obtained from the assumptions of George[a] (see text).

μ-meson energy Bev		0–2	2–4	4–6	6–8	8–10	10–12	12–14	14–16	16–18	18–20	20–22	22–24	>24
Number	Present experiment	1	6	4	1	1	1		1			1		10
	George's results	9	3.5	2.8	2.6	1.6	1.6	0.8	0.8	0.8	0.8	0.4	0.4	

[a] See reference 1.

ciable fraction of the $1p$ stars observed in an emulsion underground is due to π mesons or protons, in agreement with the conclusion reached above.

d. Photon Cross Sections

The measured energy transfer distribution given in Fig. 9 can be used along with the W-W procedure to infer photon interaction cross sections in carbon for photon energies in the range 0.1 to 10 Bev. Equation (6) can be used for this purpose and the results are shown in Fig. 10 where the points represent average values of the photon cross section over energy intervals indicated by the horizontal lines.

Photon cross sections have been measured in light nuclei up to bremsstrahlung energies of about 450 Mev. For energies well above the giant resonance region the Levinger "quasi-deuteron" model appears to account for the interactions not involving π-meson production,[19] the photodisintegration cross section per nucleon being approximately 1.6 times higher in oxygen than in deuterium.[19] The curve marked D in Fig. 10 is 12×1.6 times the measured photodisintegration cross section per nucleon in deuterium.[20] Also drawn for comparison in Fig. 10 are the curves marked π; the broken curve is 12 times the single neutral π-meson photoproduction cross section from hydrogen[21] while the solid curve is 6 times the single charged π-meson photoproduction cross section from hydrogen,[21] the nuclei in carbon being assumed to be roughly half as effective as free nucleons for charged production.[21]

When one considers the rather poor statistics in the present experiment, the agreement between the two low-energy points and the curves in Fig. 10 is as good as could be expected. As already mentioned, at least two factors could effect the accuracy of these two points; first, the detection efficiency for events in which a single π meson of energy <300 Mev is produced may be rather low, particularly for π^0 production; secondly, the estimated energy transfer (the abscissa in Fig. 10) may be low in some cases, shifting some of the events to the lower energy group. From the two high-energy points in Fig. 10 (the one at 7 Bev is based on 8 events) it is concluded that the photon interaction cross section at least does not decrease with energy and may increase for photon energies in the region of 7 Bev. This is in rough agreement with the work of Barrett *et al.*[22] who used a counter arrangement to detect high-energy interactions produced by μ mesons 1600 meters water equivalent underground. These authors inferred a photon interaction cross section $\approx10^{-27}$ cm^2/nucleon for photon energies above 5 Bev.

ACKNOWLEDGMENTS

The author wishes to thank Dr. D. C. Rose for his interest in this work and for his help in designing the electronic circuits. Mr. J. P. Bernier, of the University of Ottawa, assisted in the scintillator calibrations.

[19] Odian, Stein, Wattenberg, Feld, and Weinstein, Phys. Rev. **102**, 837 (1956).
[20] J. C. Keck and A. V. Tollestrup, Phys. Rev. **101**, 360 (1956).
[21] Schweber, Bethe, and de Hoffmann, *Mesons and Fields* (Row, Peterson and Company, Evanston, 1955), Vol. 2, pp. 150–171.
[22] Barrett, Bollinger, Cocconi, Eisenberg, and Greisen, Revs. Modern Phys. **24**, 133 (1952).

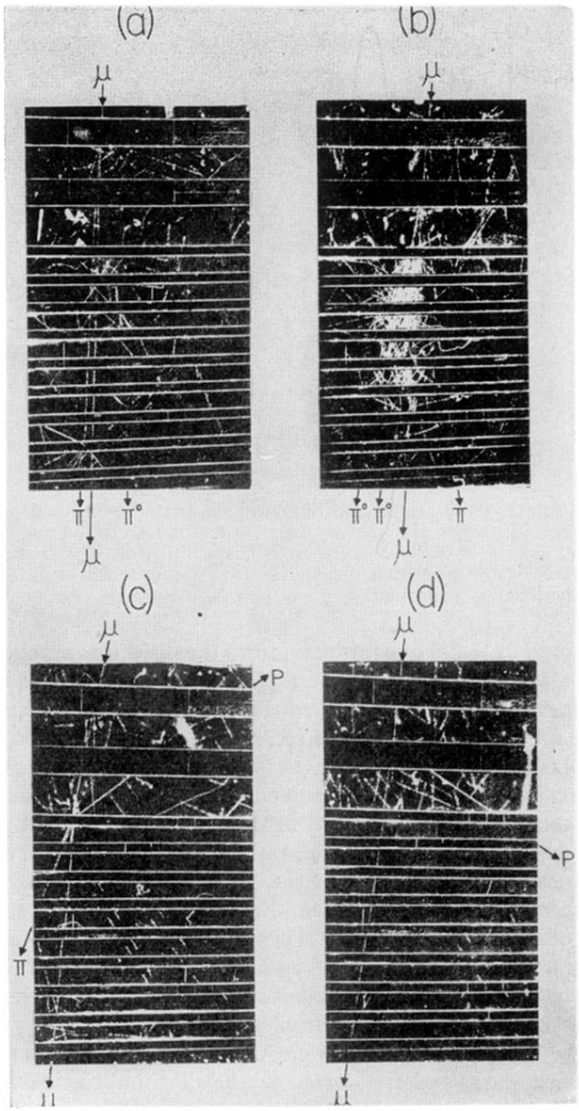

FIG. 6. Examples of nuclear interactions produced by μ mesons. (a) Interaction in the top scintillator in which one charged and one neutral π meson are produced. The charged meson interacts in the eighth plate. The third charged particle coming from the top scintillator is an electron, presumably a knock-on. (b) Interaction in the bottom scintillator in which at least one charged and two neutral mesons are produced. The energy in the electron showers $\approx$9 Bev. (c) Interaction in the top plate in which one π meson and several protons are emitted, one proton enters the bottom scintillator. (d) Interaction in the bottom scintillator in which a single proton emerges.